

Improved amplitude–frequency characteristics for T-splitter photonic crystal waveguides in terahertz regime

S. Li · H.-W. Zhang · Q.-Y. Wen · Y.-Q. Song ·
W.-W. Ling · Y.-X. Li

Received: 7 October 2008 / Revised version: 16 February 2009 / Published online: 2 April 2009
© Springer-Verlag 2009

Abstract Based on the plane-wave expansion method, we calculate TE/TM gaps of 2-D photonic crystals (PCs) with typical square lattices composed of the silicon rods in air. Using the finite-difference time-domain method, we simulate the electromagnetic field distribution of THz waves in photonic crystals T-splitters. By the improved T-splitter with a rod in the junction, we achieved the amplitude–frequency characteristics of a pass band of 84% from 1.12 to 1.22 THz and surpassed by 76% the amplitude consistency of common T-splitters. And using the finite-difference time-domain method, we demonstrated that the improved T-splitter excels a common T-splitter in the degree of separation between the two output ports. These results provide a useful guide and a theoretical basis for the developments of THz functional components.

PACS 42.79.Gn · 41.20.Jb · 42.70.Qs

1 Introduction

Terahertz (THz) radiation is a part of the electromagnetic spectrum. THz frequencies cannot clearly be classified to be either on the *electronic* side or on the *optics* side, commonly referred to as the “terahertz gap” (0.1–10 THz, $\lambda = 3$ mm to

30 μm). The THz frequency radiation has been proved as a fertile region in the electromagnetic spectrum and a powerful tool in scientific research and many applications [1, 2]. Although enormous efforts have been focused on the search for “terahertz” materials or alternative novel techniques to enable the construction of device components, much work remains. THz waves have significant transmission loss in the atmosphere [2] so waveguide-based terahertz devices have become an important foundation for the THz transmission as well as the bottle-neck for its practical applications.

Over the past few years the parallel plate waveguide (PPWG) has received much attention for its use at THz frequencies. While many groups have demonstrated various waveguides for THz applications, most of the recent work has focused on THz photonic band gap (PBG) structures [3–9]. Photonic crystals have inspired great interest recently because of their potential ability to control the propagation of waves. They can modify and even eliminate the density of electromagnetic states inside the crystal [10–13]. Such periodic dielectric structures with complete band gaps can find many applications, including the fabrication of lossless dielectric mirrors and resonant cavities for optical light [10]. A subset of the THz PBG research has included the integration of these structures into waveguides resulting in a plastic photonic fiber [3], and a dielectric waveguide grating [4]. Another useful waveguide device is a splitter, which divides the power in the input wave guide equally between two output waveguides [10]. Like the bend waveguide, the photonic band gap eliminates radiation loss and we only need to deal with the possibility of reflection. Unlike the bend waveguide, it turns out that we cannot eliminate reflections by the symmetry argument and must do something counterintuitive. We need to obstruct the output waveguides in order to increase transmission [10]. In

S. Li · H.-W. Zhang (✉) · Q.-Y. Wen · Y.-Q. Song · W.-W. Ling ·

Y.-X. Li

State Key Laboratory of Electronic Thin Film and Integrated Devices, University of Electronic Science and Technology of China, Chengdu, Sichuan, 610054, People’s Republic of China

e-mail: hwzhang@uestc.edu.cn

Fax: +86-28-83201810

S. Li

e-mail: ltriumph@163.com

this letter, we demonstrate an improved method for guiding wave around T-splitter using photonic crystal waveguides.

2 Simulation and discussion

2.1 Band gap characteristics of 2-D THz PCs with square lattices

For simplicity, we choose to study a 2-D photonic crystal of long dielectric rods in air on a square array with lattice constant of a . Their 2D photonic crystals composed of long dielectric rods in air can be realized in a practicable form by incorporating the same lattice pattern in the thin space between the two metal plates of a parallel-plate waveguide, as discussed and demonstrated in [6–9]. According to Grischkowsky's work [14], Silicon (Si) with the index of refraction (n) of 3.4176 is excellent for THz transmission due to its nondispersive nature and low absorption in THz region. So here we choose Si rods for simulation. Figure 1 shows the schematics of 2-D PC structures with typical square lattices and the circles represent the Si rods. We choose the lattice constant a to be 100 μm . Since it remains unchanged under rescaling [10] for a PBG material, we can easily assure that the guided light will be in the infrared or visible region. For example, if we choose the lattice constant a of 0.58 μm , the wavelength corresponding to the mid-gap frequency will be 1.55 μm .

Based on the plane wave expansion method [15], the band-gap dependence on the rod radius (R) has been calculated, for both the TE (electric field polarized along the axes of the dielectric columns) and TM (polarized perpendicular to the columns) PBGs in the 2-D lattice structures as shown in Fig. 1. The calculated results are shown in Fig. 2, in which it illustrates the relationship between TE/TM band gap and R . As we can see there are no complete PBGs in our calculation based on the above 2-D PC structure. It is reasonable as for its high spatial symmetry of the structure, which will lead to the degeneracy of photonic bands. This result is also consistent with the former report [10]. So under this condition, no matter how R is varied, no complete PBGs appear. Obviously the TM gaps are very sparse, which is because the isolated patches of low- ϵ regions, such as Si rods in our

Fig. 1 Schematics of 2-D PCs with typical square lattices composed of the Si rods in air background

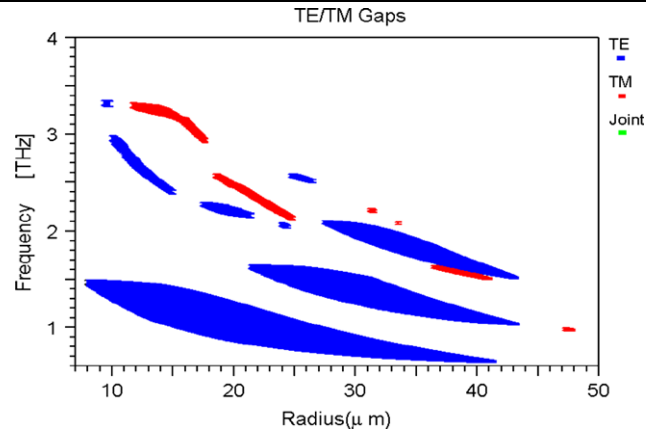
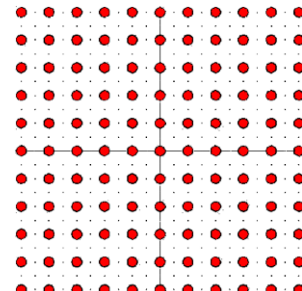


Fig. 2 Gap maps for square lattices composed of the Si rods in air background

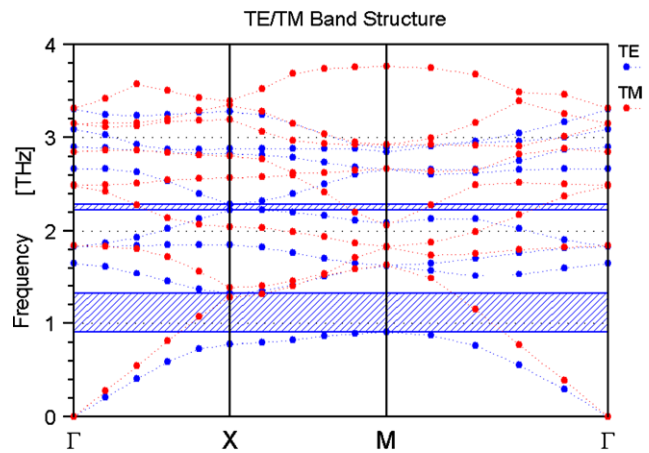


Fig. 3 TE/TM band structure for the square lattice with the arrayed Si rods with $R = 18 \mu\text{m}$ in air background

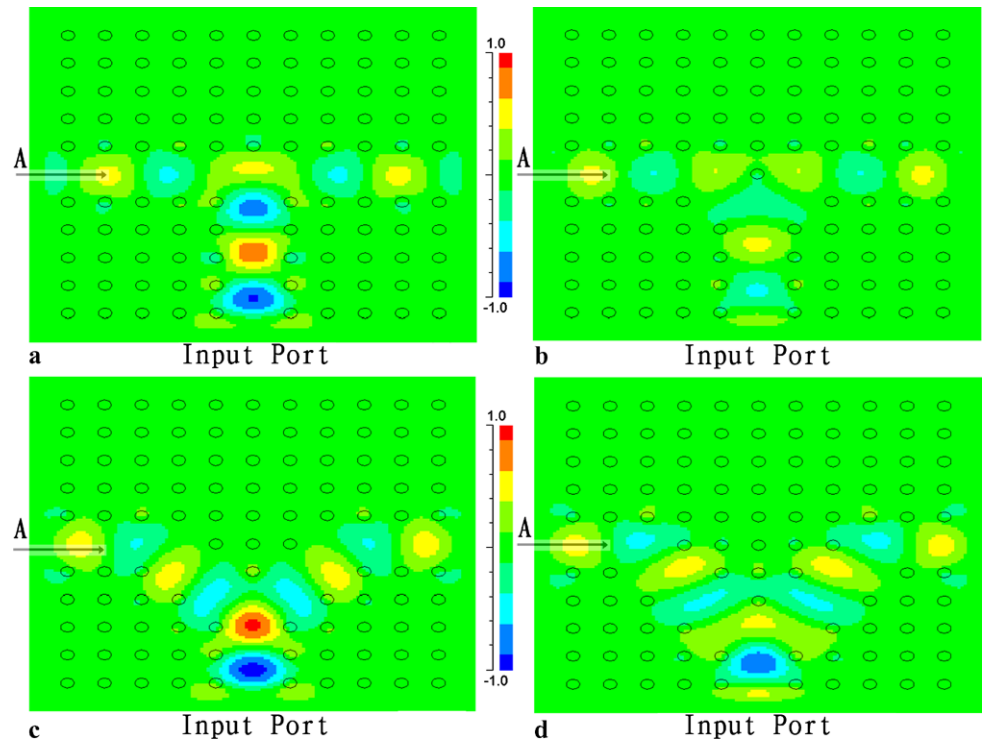
structure, would lead to the TE gaps and the connectivity of low dielectric constant regions is conducive to the TM gaps [10].

Since the TE gaps are found relatively wider with R varied from 14 to 22 μm in Fig. 2, we thus calculate the TE band-gap structure for the square PCs with $R = 18 \mu\text{m}$. The calculated results are shown in Fig. 3. As can be seen two TE band gaps namely I and II exist in two different frequency regions. Gap I is wider with a frequency range from 0.91 to 1.33 THz, while gap II is much narrower with a frequency range from 2.23 to 2.28 THz.

2.2 Electromagnetic field distribution and guided modes in 2-D THz PCs T-splitters

Figure 4 shows four different T-splitter configurations: (a) shows the common T-splitter called T0, (b) shows the T-splitter that has one rod in junction called T1, (c) shows

Fig. 4 The electric field pattern in the vicinity of the T-splitter for frequency 1.059 THz. The TE electric field is polarized along the axis of the dielectric columns. Electric field distribution of TE wave in (a) T0, (b) T1, (c) T2, and (d) T3 waveguide. The circles represent the Si rods arrayed in air with $r = 18 \mu\text{m}$



the T-splitter that has four rods in junction called T2, and (d) shows the T-splitter that has nine rods in junction called T3. The field pattern of the propagating mode can be observed by a continuous wave (CW) excitation of the guided mode. According to the previous results [11], we set the CW excitation frequency to 1.059 THz, and the corresponding electric field distribution pattern was simulated and shown in Fig. 4. As it can be clearly seen, the mode is completely confined inside the guides, and the wave travels smoothly around the sharp bend even though the radius of curvature of the bend is on the order of the wavelength [10–13].

In order to monitor the field amplitude that travels after T-splitter, we set a monitor point after the T-splitters at the position of $(-400, 0, 0)$, labeled as point A in Fig. 4. The coordinates of $(-400, 0, 0)$ is selected due to the following reasons. In principle, the position selected to monitor the signal after T-splitter should be as close as possible to T-splitter for enough of the signal amplitude. At the same time, the monitor position should be in a region with consistent structure for signal transmission. Thus from these two aspects, $(-400, 0, 0)$ is appropriate to be set as the signal monitor position. We study the transmission properties of waveguide splitters using a vector finite-difference time-domain program with quartic perfectly matched layer boundaries [15]. In our simulation, a dipole located at the entrance of the waveguide creates a pulse with a Gaussian envelope in time and the pulse time be set to lambda, when a Fourier transform is performed, the bandwidth is increased

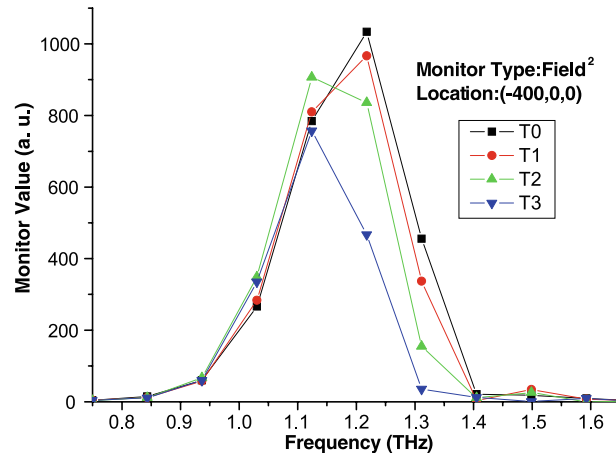
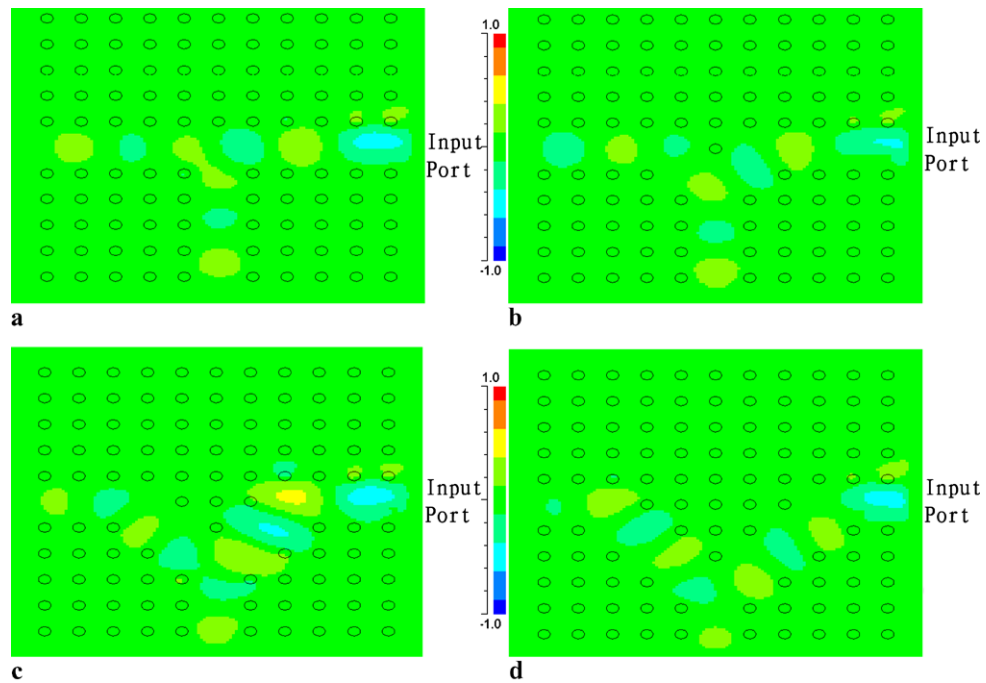


Fig. 5 The field amplitude is monitored inside the T-splitters waveguides

in the frequency domain if the pulse is narrowed in the time domain. Thus, by reducing this parameter, we increase the width of the spectral response that we can obtain in the frequency domain. Figure 5 shows the frequency dependence of field amplitude, which is monitored inside the T-splitters guides at point A. As it can be seen, four curves have similar features: field amplitude increases sharply at 0.843 THz and decreases quickly at 1.50 THz. The amplitude reaches its highest point near the frequency 1.12 and 1.22 THz, those features are determined by the structure of photonic crystals [10–13]. Obviously the four curves are different. For example, T0 first reaches its subpeak value of 785 at 1.12 THz

Fig. 6 While the input port is in the right of T-splitters, the electric field pattern in the vicinity of the T-splitter is of 1.059 THz. The electric field is polarized along the axis of the dielectric columns. Electric field distribution of TE wave in (a) T0, (b) T1, (c) T2, and (d) T3 waveguide. The circles represent the Si rods arrayed in air background at $r = 18 \mu\text{m}$



and then increases to its peak value of 1035 at 1.22 THz. For T1 its subpeak is 810 at 1.12 THz and then increases to its highest point of 965 at 1.22 THz. T2 and T3 are more special than T0 and T1 curves. That is, T2 first reaches its highest point of 905 at 1.12 THz and then decreases to its subpeak point of 835 at 1.22 THz. Similarly, T3 first reaches its highest point of 755 at 1.12 THz and then decreases to its subpeak value of 465 at 1.22 THz. Those differences are determined by the bend structure of T-splitters [10, 11].

From Fig. 5 we can also see that the pass band of T-splitters is from 1.124 to 1.22 THz. We define the amplitude–frequency characteristics consistency of pass band as δ , its value is the ratio of the subpeak amplitude comparing with that of the highest peak. So the value of δ implies the consistency of the pass band. According to Fig. 5, δ of T0, T1, T2, and T3 are 76, 84, 92, and 62%, respectively. Thus we can conclude that the consistency quality of these four configurations are T2 > T1 > T0 > T3. But considering the practical fact in signal propagation that the loss at higher frequencies is a little greater than at lower frequencies, higher transparency at higher frequencies is better. This is just the case in T1 curve. Thus considering the consistency quality as well as the demand in signal propagation, T1 is the best choice comparing with other configurations.

The function of a splitter is divides the power in an input wave guide equally between two output waveguides. A disturbance of one output port will affect the other output port. In order to explore the effect, we assumed a disturbance in the right output port of T-splitters and set the right of T-splitters to be the input port. We also simulate the field pattern of the propagating mode to observe by a continu-

ous wave (CW) excitation of the guided mode and set the frequency to 1.059 THz. We show in Fig. 6 the electric field pattern for the difference of T-splitter where 1.059 THz. Figure 6 shows trend of the left output port to gain less power while T-splitters changes from T0 to T3. In Fig. 6a, the right input can transmit to the left output without resistance. In Fig. 6b, the right input can transmit to the left output with resistance created by the rod in the junction. The difference between Figs. 6a and b is small but with the trend of gaining less power, we believed that the left output port of T1 gained less power than T0. Namely, the improved T-splitter excels a common T-splitter in the degree of separation between the two output ports.

3 Conclusion

By the improved T-splitter with a rod in the junction, we achieved the amplitude–frequency characteristics consistency of a pass band of 84% surpassing by 76% the consistency of a common T-splitter through the band from 1.12 to 1.22 THz. And the improved T-splitter excels a common T-splitter in the degree of separation between the two output ports. These results provide a useful guide and a theoretical basis for the developments of THz functional components.

Acknowledgements This work was supported by the National Basic Research Program (973) of China under Grant No. 2007CB310407, Foundation for Innovative Research Group of the NSFC under Grant No. 60721001, the International S&T Cooperation Program of China under Grant No. 2006DFA53410 and 2007DFR10250.

References

1. I. Hosako, N. Sekine, M. Patrashin et al., At the dawn of a new era in terahertz technology. Proc. IEEE **95**(8), 1611–1623 (2007)
2. A. Redo-Sanchez, X.-C. Zhang, Terahertz science and technology trends. Sel. Top. Quantum Electron. **14**(2), 260–269 (2008)
3. H. Han, H. Park, M. Cho, J. Kim, Terahertz pulse propagation in a plastic photonic crystal fiber. Appl. Phys. Lett. **80**, 2634 (2002)
4. J. Roux, F. Aquisapace, F. Garet, L. Duvillaret, J.L. Coutaz, Grating-assisted coupling of terahertz waves into a dielectric waveguide studied by terahertz time-domain spectroscopy. Appl. Opt. **41**, 6507 (2002)
5. A. Bingham, Y. Zhao, D. Grischkowsky, THz parallel plate photonic waveguides. Appl. Phys. Lett. **87**, 051101 (2005)
6. Y. Zhao, D. Grischkowsky, Terahertz demonstrations of effectively two dimensional photonic bandgap structures. Opt. Lett. **31**, 1534–1536 (2006)
7. Y. Zhao, D. Grischkowsky, 2-D THz metallic photonic crystals in parallel plate waveguides. IEEE Trans. Microwave Theory Tech. **55**, 656–663 (2007)
8. A. Bingham, D. Grischkowsky, Terahertz 2-D photonic crystal waveguides. IEEE Microwave Wirel. Compon. Lett. **18**, 428–430 (2008)
9. A. Bingham, D. Grischkowsky, THz 2-D high-Q photonic crystal waveguide cavities. Opt. Lett. **33**, 348–350 (2008)
10. J.D. Joannopoulos, R.D. Meade, J.N. Winn, *Photonic Crystals: Molding the Flow of Light*, 2nd edn. (Princeton University Press, New York, 2007)
11. A. Mekis, J.C. Chen, I. Kurland et al., High transmission through sharp bends in photonic crystal waveguides. Phys. Rev. Lett. **77**, 3787 (1996)
12. R.D. Meade, A. Devenyi, J.D. Joannopoulos, O.L. Alerhand, D.A. Smith, K. Kash, Novel applications of photonic band gap materials: low-loss bends and high Q cavities. J. Appl. Phys. **75**, 4753 (1994)
13. K.M. Ho, C.T. Chan, C.M. Soukoulis, Existence of a photonic gap in periodic structures. Phys. Rev. Lett. **65**, 3152–3155 (1990)
14. D. Grischkowsky, S. Keiding, M. van Exter, C. Fattinger, Far-infrared time-domain spectroscopy with terahertz beams of dielectrics and semiconductors. J. Opt. Soc. Am. B **7**, 2006–2015 (1990)
15. J.C. Chen, K. Li, Quartic perfectly matched layers for dielectric waveguides and gratings. Microwave Opt. Technol. Lett. **10**, 319–323 (1995)